Steel fibers reinforced grouted and fiber reinforced polymer grouted screw piles – an innovative deep foundations seismic systems

Yasser Abdelghany (Ph.D., P.Eng.)
Ministry of Transportation & Infrastructure, Victoria, British Columbia, Canada
M. Hesham El Naggar (Ph.D., P.Eng.)
Department of Civil and Environmental Engineering –The University of Western Ontario, London, Ontario, Canada

ABSTRACT
The axial and lateral monotonic and cyclic behavior of helical pile foundations was investigated and new helical screw systems suitable for seismic loadings were developed. More than one hundred full scale field load tests were conducted on instrumented helical screw piles installed in cohesive soil. The piles included: plain helical screw piles (P-HSP); grouted (G-HSPs); fiber reinforced polymer FRP-G-HSPs; and reinforced grouted RG-HSPs. The RG-HSP piles axial capacity was more than twice that for P-HSP, with minimal reduction after cyclic loading, and their lateral capacity was more than 3 times the P-HSPs capacity. A 3-D finite element model was established.

RÉSUMÉ
Le comportement monotone axiale et latérale et cyclique des fondations sur pieux hélicoïdaux ont été étudiées et de nouveaux systèmes de vis hélicoïdale adaptée pour les charges sismiques ont été développés. Plus d'une centaine à la pleine échelle des tests de charge sur le terrain ont été effectués sur des pieux instrumentés vis hélicoïdale installés dans des sols cohérents. Les piles incluses: plaine pieux vis hélicoïdale (P-HSP); injectés (G-HSP); polymère renforcé de fibres de PRF-G-HSP et renforcé injectés RG-HSP. Les pieux RG-HSP capacité axiale a été deux fois plus que pour P-HSP, avec une réduction minimale après le chargement cyclique, et leur capacité latéral a été de plus de 3 fois la capacité P-HSP. Un modèle par éléments finis 3-D a été établi.

1. INTRODUCTION

The performance of single helical anchors and group action was studied experimentally and theoretically by several researchers with regard to their installation torque and uplift resistance. However, their performance under axial compressive or lateral loading is not well characterized and their seismic performance was not investigated. The majority of the research on helical piles focuses on the load carrying capacity with little pile response to other loading modes such as cyclic loading effects or to full scale models. Among numerous researchers Clemence (1983, 1984) conducted laboratory testing investigations; Mooney et al. (1985) conducted field and laboratory testing; Hoyt (1989), Ghaly and Hanna (1992), Hoyt et al. (1995), and Ghaly and Clemence (1998) conducted theoretical and experimental testing, Puri and Vijay (1984), Ghaly et al. (1991), Huang et al. (1995), Johnston (1999), Perko (2000), and Pack (2000) conducted theoretical analyses. Rao and Prasad (1993), Prasad and Rao (1994), Shaheen and Demars (1995), and Frangoulides (2000) conducted experimental testing; Vickars and Clemence (2000) studied the performance of helical piles with grouted shafts experimentally.

2. SS175 HELICAL SCREW PILES

The SS175 pile is a segmented deep foundation system with helical steel bearing plates (helices) welded to a central steel shaft. Load is transferred from the shaft to the surrounding soil through the bearing plates. Segments or sections are joined with bolted couplings. Installed depth is limited only by soil resistance. A helical bearing plate or helix is one pitch of a screw thread. All helices regardless of their diameter have a standard 75 mm pitch (Fig.1). The helices have true helical shape and therefore, they do not auger into the soil but rather screw into it with minimal soil disturbance.

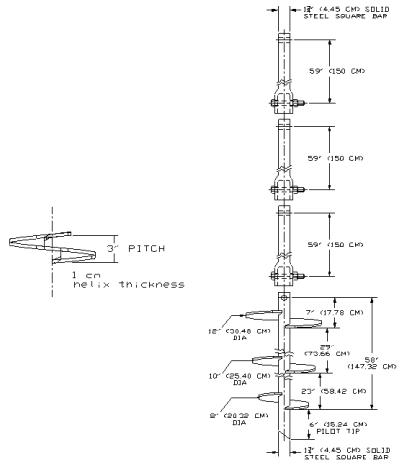

Figure.1. Schematic of an SS 175 AB Chance Helical Screw Foundation System.

3. RESEARCH OBJECTIVES AND METHODOLOGY

The main research objectives are highlighted in the following:

1. Develop new configurations of helical screw piles that can perform well under cyclic loadings.
2. Monitor the load transfer mechanism for helical screw piles with different configurations
3. Investigate the correlation between the torque of installation and piles axial compression capacities
4. Develop a separate cyclic framework capable of testing helical screw piles under axial and lateral cyclic loading

The research methodology included the evaluation of the monotonic and cyclic performance of the SS175 pile under axial and lateral loading in a layered soil profile through more than one hundred full scale field load test on twenty three SS175 helical screw piles. Twenty piles were instrumented with strain gauges distributed along the lead section length. The helical screw piles lead section had three tapered helices 30 cm, 25 cm and 20 cm from top to bottom. In this study, extension segments of 1.5 m and 2.1 m length were added to the lead section during installation to reach the desired bearing soil stratum. The experimental work proceeded through three consecutive stages of full scale field load testing under monotonic and cyclic axial and lateral loading.

4. SOIL INVESTIGATION

There is numerous soil investigation data about the site in which the piles were installed but still two boreholes were conducted as part of the current study, within the area where the piles were to be installed and load tested. The two boreholes located 16.6 meters apart and both at the middle of the pile load testing area. The two boreholes were advanced to depth 9.6 to 9.8 meters by a power auger machine equipped with conventional soil sampling equipment. Standard penetration tests were performed at frequent intervals of depth; the results were recorded on the borehole logs as N values. Five Shelby tube samples were recovered from both boreholes. Also, split-spoon samples were stored in airtight containers, which were transferred to the laboratory for classification. Borehole 1 shows silt and clayey silt overlying stiff to very stiff clayey silt to silty clay layers reaching a very dense fine to medium sand at 8.5 m. The water table at completion was encountered at a depth of 5.2 m below the ground surface. Borehole 2 shows silt and clayey silt layers overlying stiff to very stiff silty clay to clayey silt till reaching a very dense fine to medium sand at 9 m approximately. The water table at completion was measured at 6.7 m below the ground surface. Shelby tube samples of diameter 75 mm were extracted at the planned depths of the helices of the test helical piles, in order to properly define the bearing strata. Two samples were recovered at depths 3.65-4.25 m (12-14 ft) and 4.9-5.5 m (16-18 ft) in borehole 1. Three samples were recovered at depths of 2.15-2.75 m (7-9 ft), 2.75-3.35 m (9-11 ft), and 3.35-3.95 m (11-13ft) in borehole 2. The N values were corrected according to ASTM D 1586. The unconsolidated undrained (UU) triaxial strength is applicable where the pile loading is assumed to take place so rapidly that there is insufficient time for the induced pore-water pressure to dissipate and for consolidation to occur during the loading period, which represents the pile loading conditions in this study. The procedure of ASTM (D 2850-95 Re-approved 1999) was conducted on six samples.

Table 1. Boreholes Shelby Tubes Samples Soil Properties

Property	BH1S1	BH1S2	BH2S1	BH2S2
C_U (kPa)	40	100	70	50
W_C (%)	15.3	12	12	17
E (kPa)	15000	50000	45000	20000
Depth **(**m)	3.65-4.25	4.90-5.5	2.15 -2.75	3.35-3.95

Note: BH1S1 – Borehole 1 Sample No. 1; BH1S2– Borehole 1 Sample No. 2

5. GROUT TESTING AND EVALUATION

A series of compression and splitting tensile strength tests were conducted on samples at ages 7 and 28 days. Three different grout types were used the MS MICROPILE grout, PT PRECISION grout, and MASTERFLOW 1341. The ASTM C39 and CSA A-23.13 were followed during the loading tests. Twelve 200 x 100 mm (8 x 4 in) cylinders were prepared using the MS MICROPILE grout. Another fourteen cylinders were prepared seven using the PT PRECISION grout, and seven using the MASTERFLOW 1341 grout. Three cylinders of each group were prepared plain (No additives) and the remaining four were prepared by mixing 1% of NOVOCON 0730 30mm (1.18 in.) length, 0.7 mm (0.0276 in.) diameter steel fibers to increase their splitting tensile strength. The 14 cylinders were tested after 28 days. Thirty 50 x 50 mm cubes were prepared: fifteen using the PT PRECISION grout and fifteen using the MASTERFLOW 1341. Six cubes of each group were prepared plain (No additives) and the remaining nine were prepared by mixing 1% of the NOVOCON 0730 steel fibers to study the effect of fibers on the compression strength of the grout. All cubes were cured in the moisture room and were tested after 28 days. Figure 2a presents the typical cylinders behavior without (left) and with steel fibers (right) after the splitting test, in which the steel fibers have increased the splitting tensile strength of the PT PRECISION and the MASTERFLOW 1341 grout by 42% and 20% respectively on average. Figure.2b presents the compression strength test on the cubes without (left) and with steel fibers (right) in which the steel fibers have increased the compressive strength of the PT PRECISION and the MASTERFLOW 1341 grout by 51% and 33% respectively on average.

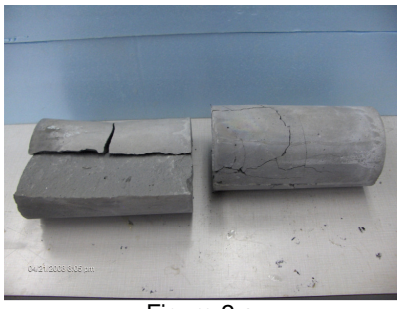

Figure 2.a

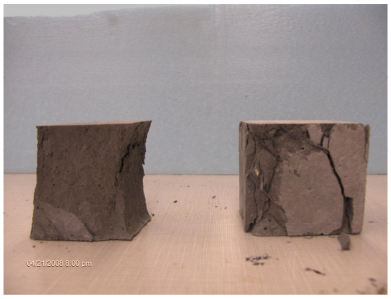

Figure 2.b

6. HELICAL SCREW PILES, INSTRUMENTATION AND INSTALLATION TECHNIQUES

Twenty three piles SS175 Chance helical screw square shaft piles system were installed and load tested, in which twenty were instrumented in advance. The piles are grouped as follows: seven plain helical screw piles (P-HSPs), four grouted helical screw piles (G-HSPs); four grouted reinforced helical screw piles (RG-HSPs), and eight fiber reinforced polymers grouted helical screw piles (FRP-G-HSPs). In addition, the inline torques versus the installation depth of forty seven plain helical screw piles, used as reaction piles, is also recorded. To determine the axial load distribution along the pile, and more specifically, the load taken by each helix, strain gauges were attached to the shaft of the lead section. Twenty 1.5 m (5 ft) length lead sections were instrumented to cover twenty instrumented helical piles. Eleven lead sections were instrumented by six strain gauges labeled from one to six, in which strain gauge number one is from the pilot side, near bottom helix, and strain gauge number six is near the top

helix. The strain gauges were attached to the shaft very close to the helices, at a distance approximately 3 cm above and below the helical bearing plate. The remaining nine lead sections were instrumented with eight strain gauges: six strain gauges close to the helices and two strain gauges were installed on the shaft at the mid distance on the shaft between each two helices. Fig. 3 shows a schematic diagram illustrating the strain gauges locations on the lead section shaft. Strain gauges #1, #3 and #5 are located below each helix; strain gauges #2, #4, and #6 are located above each helix. The strain gauges labeled as A and B were located in the middle distance between the helices. This configuration allowed monitoring the load transfer on the helices and the shaft between the helices. Fig. 4.a shows photographs for a grooved lead section where a pair of strain gauges installed close to a helix. The strain gauge resistance was measured after the lead wires were soldered to the gauges to ensure that they working properly. Fig. 4.b. shows a photograph for some instrumented piles after all gauges and wires were protected with five minute epoxy and wrapped with several layers of electric and duct tapes to reduce abrasion damage caused by the piles installation procedures.

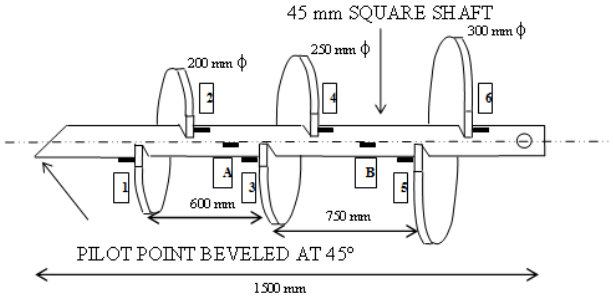

Figure.3. Schematic of lead section instrumentation with strain gauges

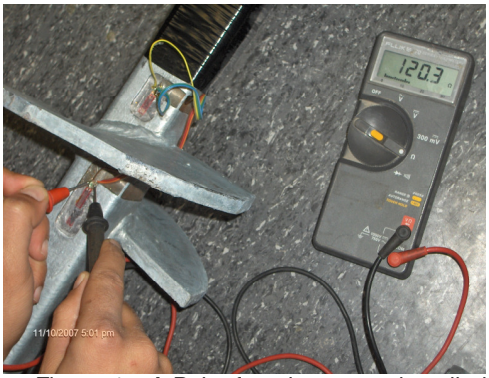

Figure 4.a A Pair of strain gauges installed and the resistance of the strain gauge is measured with an Ohm-meter

Figure 4.b. Finished instrumented lead sections

7. PILE INSTALLATION AND TORQUE /LOAD CAPACITY RELATIONSHIP

The twenty three helical piles were installed and tested under axial and lateral monotonic and cyclic loadings. In addition, forty seven helical piles were installed as reaction piles. The installation torque was recorded for all piles. The instrumented piles were installed in three stages. Fig. 5.a shows a typical preparation for an instrumented pile lead section-extension connection. Fig. 5.b shows an installation of an FRP-G-HSP. The capacity of the helical screw pile may be estimated based on the relationship between the installation torque and its ultimate capacity. The principle is that the resistance to installation (defined by installation energy or torque) increases as the helical plates is installed into increasingly stronger soils. Likewise, the higher the installation torque, the stronger the soil and thus the higher is its bearing capacity and consequently the axial capacity of the installed HSP. Hoyt and Clemence (1989) proposed the following formula for the torque/helical pile capacity relationship: Hoyt and Clemence (1989) recommended K_t = 33 m^{-1} (10 ft^{-1}) for square shaft HSP of square side dimension smaller than 89 mm. The value of K_t may range from 10 to 66 m^{-1} depending on soil conditions, shaft size and shape, helix thickness, and application (tension or compression loading).

$$Q_u = K_t T \quad (1)$$

Where Qult is the ultimate capacity [kN (lb)];
K_t is an empirical torque factor [m^{-1} (ft^{-1})]; and
T is the average installation torque along last 1 m of installation (last 3 ft) [kN.m (lb.ft)].

Figure.5.a. Typical preparation of lead section – extension connection


Figure. 5.b. FRP-G-HSP installation (internal SS175 shaft – external FRP 3m tube).

8. AXIAL MONOTONIC AND CYCLIC TESTING SETUP AND TESTING RESULTS

The axial monotonic and cyclic testing procedures and the interpretation of the results of the axial load tests on twenty instrumented helical screw piles are presented under this section. Fig. 6 shows a photograph for the axial cyclic loading test. The load was exerted through a hollow cylinder hydraulic jack with 100 ton advance capacity and 68 ton retract capacity, and 150 mm stroke connected to a hydraulic pump. The load was recorded through an interface load cell 1240-AF-200K-B of 900 kN capacity. The pile head axial displacement was measured through four HLP 190/FS1/100/4K linear displacement transducers (LDTs) with an accuracy of 0.01 mm. The displacement average was considered in the data analysis in an attempt to overcome any inaccuracies.

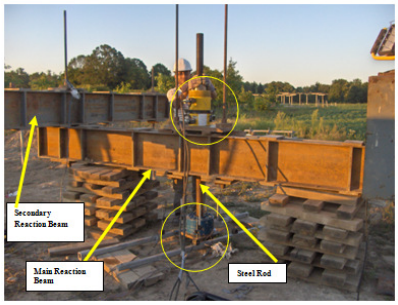

Figure.6.Axial cyclic loading setup

The load cell and LDTs were connected to the data acquisition system. Each instrumented pile was subjected to an initial compression

test, followed by a minimum of fifteen cycles of axial loading. A final compression test was conducted after the completion of cyclic loading to examine the piles capacity and performance characteristics during and after cyclic loading. Furthermore, the load transfer mechanism along the pile length was analyzed from the strain gauge records. The spacing between the test and reaction piles complied with ASTM D-1143 and ASTM D-3689.

There exist numerous failure criteria that are used for different pile types and in different building codes. Perhaps the first criterion ever formally proposed, which is still widely accepted by engineers is the one suggested by Terzaghi (1940); for practical purposes, the ultimate load should be defined as that which causes a settlement of one-tenth of the pile diameter or width. The failure criteria place the ultimate load within the nonlinear region of the load-movement curve to ensure that once a suitable factor of safety is applied, the design load of the pile should lie within the initial linear region of the curve. This will yield predictable load-displacement behavior and avoid any abrupt settlement. The axial pile load tests were conducted according to the ASTM D-1143 standard test method for piles under static axial compression load and under axial cyclic load. The quick testing method has become popular within the geotechnical community and more specifically has been used successfully to test helical piles. ASTM D 1143 specifies that test loads are applied in increments of 10 to 15% of the proposed design load with constant time interval increments of two and half minutes. Smaller increments, longer time intervals, or both can be used. In this study, loads were applied in increments of 10% of the expected design load with a constant time of 2.5 minutes. Samples of the axial loadings testing results are presented in figures 7 to 11.

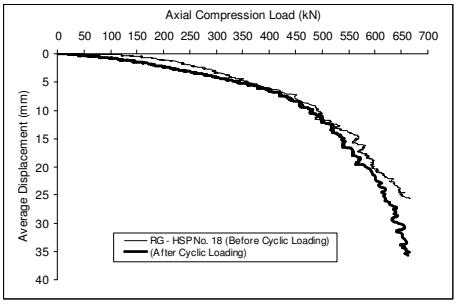

Figure.7. Load-displacement curves for RG-HSP 18 before and after cyclic loading

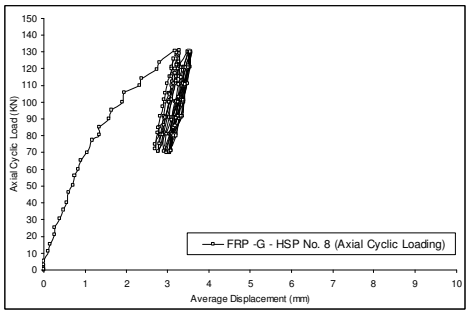

Figure. 8. FRP-G-HSP 8 axial cyclic load versus displacement

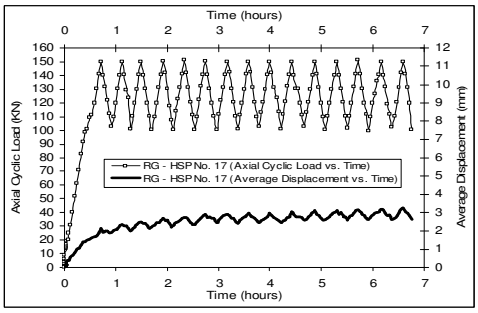

Figure.9. RG-HSP 17 axial cyclic load and displacement versus time

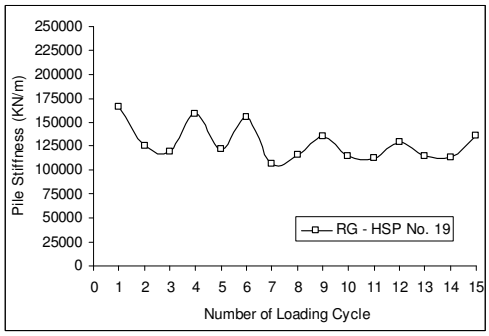

Figure. 10. RG-HSP 19 Pile Stiffness versus number of loading cycles

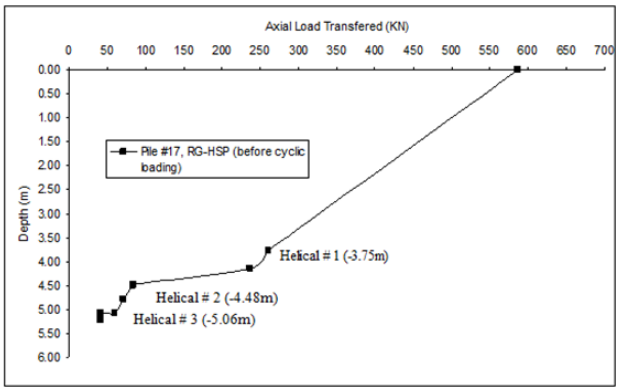

Figure.11. RG-HSP 17 axial load transfer

9. LATERAL MONOTONIC AND CYCLIC TESTING SETUP AND TESTING RESULTS

This section presents the lateral monotonic and cyclic testing procedures, including the mechanism that facilitates lateral monotonic and cyclic loading of piles. The load testing results for plain helical screw piles (P-HSP), grouted helical screw piles (G-HSP), fibre reinforced polymer grouted helical screw piles (FRP-G-HSP) and reinforced grouted helical screw piles (RG-HSP). Twenty piles were subjected to lateral loading. An initial lateral load test was performed on each pile, followed by fifteen cycles of lateral loading. After the completion of cyclic loading, each pile was subjected to a monotonic lateral load test to determine the pile lateral capacity after cyclic loading. The test setup was composed of three main steel reaction beams, each was 4.25 m long, 0.3 m wide, and 0.3 m deep. The main reaction beam was placed on the ground and was anchored to two reaction piles. To provide additional reaction mass, the other two reaction beams were placed on the ground behind the main reaction beam on the opposite side of the

Figure.12.b. Lateral loading setup zoom-in for the hydraulic jack–load cell and the four LDTs setup.

The pile lateral load-displacement curve can be used to evaluate the pile's performance under lateral loading and to assess its ultimate capacity. A generally accepted ultimate lateral load criterion is defined as the load that corresponds to a lateral displacement at the pile head equal to 6.25 mm (Prakash and Sharma, 1990). Samples of the lateral results are presented in figures 13 to 16.

Figure.12.a. Lateral loading setup

Figure.13. FRP-G-HSP with external grout separation between the FRP tube& external grout during lateral testing

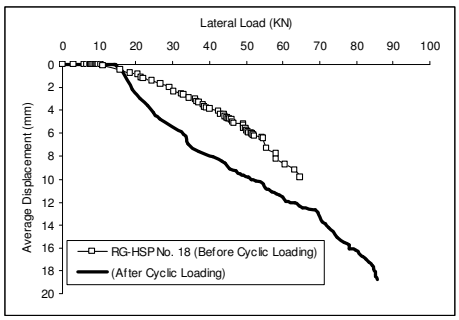

Figure.14. Stage 3 – RG-HSP 18 lateral load-displacement (before and after cyclic loading)

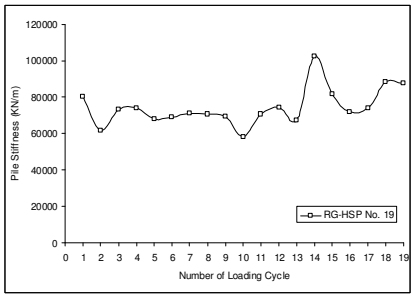

Figure.15. Stage 3 – RG-HSP 19 stiffness variation with number of loading cycles.

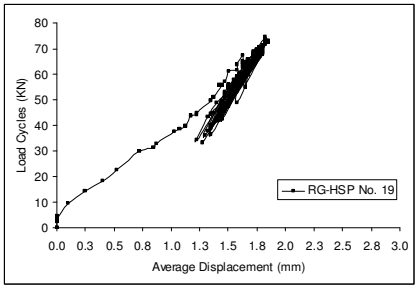

Figure. 16. Stage 3 – RG-HSP 19 lateral cyclic load-displacement curve

10. SUMMARY AND CONCLUSIONS

The primary objective of this research was to evaluate the monotonic and cyclic performance of the helical piles foundation system in selected soils under axial and lateral loading conditions. A comprehensive investigation was conducted including: literature review, full-scale load testing of instrumented piles. More than one hundred full-scale load test on twenty three helical piles with three-helix piles were tested as part of this study. All tests were performed in accordance with the appropriate ASTM standards. The relationship between the installation torque and the ultimate capacity of the piles was assessed. Twenty of the twenty three piles lead sections were instrumented with strain gauges, a good portion were able to produce the usable data to generate the axial load transfer curves for the different piles. In addition, a new cyclic loading full scale test setup was provided for the axial cyclic and the lateral cyclic testing, which is under patent rights. Three different types of grout (MS Micropile, MASTERFLOW 1341, and PT PRECISION grout) were used in the piles installation. Furthermore, different helical piles geometries were tested. The SS175 plain helical screw piles (P-HSP), the grouted helical screw piles (G-HSP), the fibre reinforced polymer grouted helical screw piles (FRP-G-HSP) in which the piles were encased in FRP tubes. The FRP-G-HSP piles were installed by two different techniques; one in which the grout is provided only inside the tube and the other in which the grout was provide inside and outside the tube to increase the friction component with the soil. Finally, a grouted reinforced column (RG-HSP), in which steel fibers were mixed to the grout to increase its tensile strength, was introduced. The interpretation of the results obtained from the different parts of this investigation has led to several conclusions. The most significant of which are presented below.

10.1 Axial Monotonic and Cyclic Full Scale Loading Tests: Based on the axial load tests and their analysis, the following conclusions can be drawn:

1. The piles axial compression capacities were found to be proportional to the installation torque. Therefore, the empirical torque correlation factor KT can be used to predict the pile capacity of the plain helical screw piles (P-HSP). The value of KT of 33 m-1 is a sound value for piles in clayey silt to silty clay soils.

2. The Terzaghi (1940) failure criterion (10% of the average helices diameter) was adopted to obtain the ultimate axial compression capacities of all tested piles. It was found that the capacity of piles before cyclic loading varied between 240-282 kN for P-HSPs, 321-341 kN for G-HSPs, 235-327 kN for FRP-G-HSPs with internal grout, 303-460 kN for FRP-G-HSP piles of internal and external grout, and 431-650 kN for RG-HSP piles.

3. The capacity of piles after 15 load cycles varied between 278-313 kN for P-HSPs, 280-422 kN for G-HSPs, 264-483 kN for FRP-G-HSPs with internal grout, 290-338 kN for FRP-G-HSPs of internal and external grout, and 553-617 kN for RG-HSPs.

4. Minimal degradation of piles stiffness occurred after the 15 loading cycles, with the reinforced grouted helical screw piles (RG-HSP) presented the best stiffness performance.

5. The reinforced grouted helical screw piles (RG-HSP) showed the highest axial ultimate compression capacity of all different geometry tested helical piles. This confirms the beneficial effect of the reinforced grouted shaft on increasing the axial capacity and enhancing the seismic performance.

6. The load transfer mechanism analyzed from the measured strain data showed about 55% shaft resistance in case of the reinforced grouted helical screw piles, and an average of 14% in case of plain helical screw piles.

10.2. Lateral Monotonic and Cyclic Full Scale Loading Testing: Based on the lateral load tests and their analysis, the following conclusions can be drawn:

1. The ultimate capacities of the tested piles were obtained as the load at pile head deflection of 6.25 and 12.5 mm (i.e. two different failure criteria). The P-HSPs had negligible lateral capacity. The capacity of the G-HSPs varied between 14 and 26 kN, and from 7.5 to 12 kN for FRP-G-HSPs with internal grout and from 20 to 64 kN for FRP-G-HSPs with internal and external grout. The RG-HSPs ranged from 42 to 80 kN.

2. The lateral capacity of most pile configurations degraded due to the cyclic loading. However, the RG-HSPs showed a small reduction, and in some cases some increase, in the capacity after the cyclic loading. The (RG-HSP) presented the best stiffness performance during the 15 loading cycles.

REFERENCES

Abdelghany, Y., 2008. Monotonic and Cyclic Behavior of Helical Screw Piles Under Axial and Lateral Loading. Ph.D. thesis, The University of Western Ontario, Canada.

ASTM International. Standard Test Method for Individual Piles Under Static Axial Tensile Load. Designation D3689-90 (Reapproved 1995). West Conshohocken, PA, USA.

ASTM International. Standard Test Method for Individual Piles Under Static Axial Compressive Load. Designation D 1143–81 (Reapproved 1994). West Conshohocken, PA, USA.

Clemence S. P., 1984. Dynamic uplift capacity of helical anchors in sand. National Conference Publication- Institution of Engineers in proceedings of Fourth Australia-New Zealand Conference on Geomechanics: Geomechanics-Interaction, n84/2: 88-93.

Clemence S. P., 1983. Dynamic uplift capacity of helical anchors in sand. Civil Engineering for Practicing and Design Engineers, 2(3): 345-367.

Frangoulides, A.C., 2000. Model testing of continuous helical displacement piles. Ground Engineering, 33(12): 34-37.

Ghaly, A.M., Clemence, S.P., 1998. Pullout performance of inclined helical screw anchors in sand. Journal of Geotechnical and Geoenvironmental Engineering, ASCE, 124(7): 617-627.

Ghaly, A.M. and Hanna, A.M, 1992. Stress and strains around helical screw anchors in sand. Soils and Foundations, 32(4): 27-42.

Ghaly, A.M. and Hanna, A.M., 1991. Experimental and theoretical studies on installation torque of screw anchors. Canadian Geotechnical Journal, 28(3): 353-364.

Hoyt, R.M. Seider, G., Reese, L.C., Wang, S.T., 1995. Buckling of helical anchors used for underpinning. Geotechnical Special Publication, n 50, Foundation upgrading and repair for infrastructure improvement: 89-108.

Hoyt, R. M., and Clemence, S.P., 1989. Uplift capacity of helical anchors in soil. Proc. of the 12th International Conference on Soil Mechanics and Foundation Engineering. Rio de Janerio, Br., Vol. 2: 1019-1022.

Huang, F., Mahmoud, I., Joolazadeh, M., and Axten, G.W., 1995. Design considerations and field load tests of a helical anchoring system for foundation renovation. Geotechnical Special Publication, n 50, Foundation upgrading and repair for Infrastructure Improvement: 76-88.

Johnson, K., Lemcke, P., Karunasena, W., and Sivakugan, N. 2006. Environmental Modelling and Software, Vol. 21: 1375-1380.

Johnston, R. J., 1999. Helical piling foundations in Juneau, Alaska. Proceedings of the 10th International Conference on Cold Regions Engineering: 731-736.

Mooney, Joel S., Adamczak, S.J., Clemence, S.P., 1985. Uplift capacity of helical anchors in clay and silt. ASCE Convention Conference Proceedings, Detroit, MI: 48-72.

Pack, J.S., 2000. Design of helical piles for heavily loaded structures. Geotechnical Special Publication, n 100: 353-367.

Perko, H.A., 2000. Energy method for predicting installation torque of helical foundations and anchors. Geotechnical Special Publication, n 100: 342-352.

Prakash, S. and Sharma, H.D., 1990. Pile foundations in engineering practice. John Wiley and Sons, New York, N.Y.

Prasad, Y.V.S.N., Rao, N.S., 1994. Pullout behaviour of model pile and helical pile anchors subjected to lateral cyclic loading. Canadian Geotechnical Journal, 31(1): 110-119.

Puri, and Vijay K., 1984. Helical anchor piles under lateral loading. Laterally Loaded Deep Foundations: Analysis and Performance, Conference, Kansas City, Mo, USA and ASTM Special Technical Publication: 194-213.

Rao, N.S.; Prasad, Y.V.S.N, 1993. Estimation of uplift capacity of helical anchors in clay. Journal of Geotechnical Engineering, 119(2): 352-357.

Rao, N.S., and Prasad, Y.V.S.N., 1991. Estimation of uplift capacity of helical anchors in clays. Journal of Geotechnical Engineering, 199(2): 352-357.

Rao, N.S., Prasad, Y.V.S.N., Shetty, M.D., and Joshi, V.V., 1989. Uplift capacity of screw anchors. Geotechnical Engineering, 20(2): 139-159.

Rao, N.S. and Venkatesh, K.H., 1985. Uplift behaviour of short piles in uniform sand. Soils and Foundations, 25:1-7.

Shaheen, W.A., Demars, K.R., 1995. Interaction of multiple helical earth anchors embedded in granular soil. Marine Georesources and Geotechnology, 13(4): 357-374.

Terzaghi, K., 1940. Theoretical soil mechanics. Wiley, New York.

Vickars, R.A., Clemence, S.P., 2000. Performance of helical piles with grouted shafts. Geotechnical Special Publication, n 100:327-341